Conformation of the Mushroom Toxin β-Amanitin in the Crystalline State†

Edward C. Kostansek, William N. Lipscomb,* R. Rogers Yocum, and William E. Thiessen

ABSTRACT: A single crystal X-ray diffraction analysis of β-amanitin, a bicyclic octapeptide toxin isolated from the poisonous mushroom *Amanita phalloides*, shows that the molecule has distinct regions of hydrophilic and hydrophobic residues and two 18-membered rings. The study confirms the proposed chemical sequence and the configuration of the residues. All eight peptide groups are in the trans conformation. Four intramolecular hydrogen bonds, two strong and two weak, occur in the structure. The toxin cocrystallizes with seven water and three ethanol molecules and participates in an extensive hydrogen-bonding network. The crystal structure was solved by direct methods. The space group is $P2_12_12_1$, and unit cell dimensions are a = 14.004 (3), b = 14.943 (3), and c = 30.794 (7) Å.

Approximately 95% of all deaths by mushroom poisoning are caused by the green death cap, *Amanita phalloides* (Wieland & Wieland, 1972). Three families of toxic compounds have been isolated from this mushroom, the amatoxins, the phallotoxins, and the phallolysins (Faulstich & Weckauf-Bloching, 1974). Of these three groups, it is the amatoxins which account for the extreme toxicity of this mushroom for humans. The amatoxins act by killing hepatocytes and secretory cells of the kidney via inhibition of DNA-dependent RNA polymerase II (Cochet-Meilhac & Chambon, 1974).

The chemical structures of the most abundant amatoxins, α- and β-amanitin, have been elucidated (Wieland & Wieland, 1972). They are bicyclic octapeptides containing the unusual amino acids, hydroxylated isoleucine, 6-hydroxytryptophan, and a cysteine sulfoxide transanular bridge (see Figure 1). Since the original publication three corrections in the details of the structure have been made. An amino acid residue originally described as β-methyl-γ,δ-dihydroxyisoleucine was changed to γ,δ-dihydroxyisoleucine (Wieland & Gebert, 1966). A stereochemical error in this residue was corrected in a subsequent study (Gieren et al., 1974). Finally, the original thioether of the transanular bridge was replaced by a sulfoxide (Faulstich et al., 1968).

Because of the chemical complexity of the molecule and the apparent importance of overall conformation for the mode of action of the toxin (Faulstich et al., 1973), an X-ray crystallographic structural study was undertaken. Both α- and β-amanitin had been crystallized (Wieland et al., 1949), but in both cases the crystals were extremely fine asbestos-like needles which were unsuitable for X-ray analysis. This paper describes in detail the successful crystallization of β-amanitin and the elucidation of its three-dimensional crystal structure by X-ray diffraction. A preliminary report of this work has been published (Kostansek et al., 1977).

Experimental Section

The free acid form of β-amanitin was purified from dried *Amanita phalloides* as described in the accompanying paper (Yocum, 1978). About 200 mg of the purified material was dissolved in 10 mL of 95% ethanol by warming to 50 °C in a 1-L round-bottomed flask. The flask was then left opened at room temperature (about 20 °C). In 24 h, several crystals measuring up to approximately 0.5 × 2 mm had grown. The crystallization was repeatable using a second, independent batch of β-amanitin. A photomicrograph of the β-amanitin crystals is shown in Figure 2.

The crystals have the symmetry of the orthorhombic space group $P2_12_12_1$. The unit cell has dimensions a = 14.004 (3), b = 14.943 (3), and c = 30.794 (7) Å (λ = 1.54178 Å) and contains 4 cyclopeptide molecules and approximately 40 water and ethanol molecules. A crystal for data collection, measuring 0.23 × 0.37 × 0.63 mm, had to be sealed in a glass capillary with a small amount of mother liquor in order to prevent deterioration. The integrated intensities of 4104 independent reflections ($2\theta_{max}$ = 105°) were measured with graphite monochromated Cu K_α radiation on an automated four-circle diffractometer. The data were collected using 1.5° ω scans (1°/min) with 20-s background counts at each end of the scan. Three reference reflections, measured every 50 reflections, decayed only a few percent during the entire data collection. An automatic orientation check was utilized every 200 reflections. Reflection intensities were corrected for background, polarization, and Lorentz effects. Those 3395 reflections (83%) which had values of $F_o \geq 3\sigma(F_o)$ were considered to be observed and were included in the refinement.

Structure Determination and Refinement. The structure was solved using the weighted multiple solution tangent for-

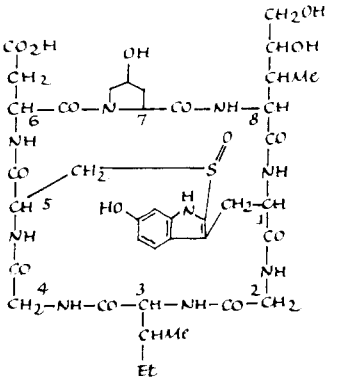

FIGURE 1: Chemical structure of β-amanitin.

† From the Gibbs Chemical Laboratory (E.C.K. and W.N.L.) and the Biological Laboratories (R.R.Y.), Harvard University, Cambridge, Massachusetts 02138, and the Chemistry Division, Oak Ridge National Laboratory, Oak Ridge Tennessee 37830 (W.E.T.). *Received January 9, 1978.* Research sponsored in part by the Energy Research and Development Administration under contract with Union Carbide Corporation. This research was supported by National Institutes of Health Grant GM-06920.

0006-2960/78/0417-3790$01.00/0

TABLE I: Fractional Atomic Coordinates × 10^4.[e]

atom[d]	x	y	z	atom[d]	x	y	z
1N	−977 (8)	3604 (7)	4463 (3)	6CG	−1373 (11)	4779 (10)	3172 (4)
1CA	−943 (10)	2662 (9)	4387 (4)	6OD1	−1371 (8)	4485 (7)	3551 (3)
1CB	−1498 (10)	2455 (8)	3954 (4)	6OD2	−2141 (8)	4656 (8)	2953 (4)
1CG	−1367 (9)	1546 (8)	3774 (4)	6C	529 (11)	5141 (9)	3659 (4)
1CD1	−1103 (10)	1362 (9)	3355 (4)	6O	722 (8)	4518 (6)	3900 (2)
1CD2	−1558 (10)	700 (9)	3983 (4)	7N	401 (9)	5981 (7)	3812 (3)
1NE1	−1132 (9)	456 (8)	3282 (4)	7CA	607 (11)	6126 (10)	4277 (4)
1CE2	−1418 (12)	12 (9)	3674 (4)	7CB	483 (14)	7138 (10)	4313 (5)
1CE3	−1858 (12)	450 (10)	4391 (4)	7CG	765 (16)	7507 (12)	3883 (5)
1CZ2	−1524 (13)	−863 (10)	3753 (5)	7OD1	1771 (11)	7504 (11)	3848 (4)
1CZ3	−1988 (13)	−436 (12)	4472 (5)	7CD2	372 (14)	6813 (9)	3582 (4)
1CH2	−1844 (15)	−1107 (12)	4155 (5)	7C	19 (11)	5589 (10)	4577 (4)
1OT2	−1905 (13)	−2000 (7)	4272 (4)	7O	414 (8)	5344 (8)	4925 (3)
1C	42 (9)	2275 (9)	4413 (4)	8N	−873 (8)	5424 (7)	4498 (3)
1O	123 (8)	1499 (7)	4565 (4)	8CA	−1485 (10)	5006 (9)	4802 (4)
2N	778 (7)	2701 (8)	4253 (3)	8CB	−2540 (11)	5244 (9)	4731 (5)
2CA	1712 (10)	2424 (11)	4311 (4)	8CG1	−3102 (13)	5312 (11)	5157 (5)
2C	2387 (10)	2495 (9)	3944 (4)	8CG2	−3046 (12)	4642 (11)	4366 (5)
2O	2109 (7)	2886 (7)	3603 (2)	8OD1	−2654 (9)	5964 (8)	5448 (4)
3N	3262 (7)	2200 (8)	3998 (3)	8CD2	−4161 (13)	5537 (13)	5125 (6)
3CA	4041 (10)	2281 (11)	3688 (4)	8OE1[a,c]	−4532 (24)	5611 (26)	5535 (12)
3CB	4938 (10)	1893 (10)	3852 (4)	8OE2[a,c]	−4766 (25)	4916 (25)	4879 (10)
3CG1	5310 (11)	2439 (12)	4248 (5)	8OE3[a,c]	−4371 (38)	6344 (28)	4871 (13)
3CG2	5731 (12)	1816 (14)	3513 (5)	8C	−1345 (10)	3980 (9)	4815 (4)
3CD	6040 (12)	1905 (15)	4527 (5)	8O	−1617 (8)	3532 (6)	5138 (3)
3C	3736 (11)	1813 (10)	3258 (4)	W1	2186 (14)	1469 (9)	1177 (3)
3O	3394 (8)	1091 (6)	3255 (3)	W2	−1893 (17)	−2391 (10)	5136 (4)
4N	3821 (7)	2335 (8)	2898 (3)	W3[b]	3583 (20)	−306 (17)	3923 (6)
4CA	3489 (12)	2001 (11)	2466 (4)	W4[c]	−4085 (18)	4704 (24)	3283 (9)
4C	2470 (10)	2182 (9)	2379 (4)	W5[c]	306 (31)	5831 (32)	5879 (12)
4O	2120 (7)	1968 (8)	2034 (3)	W6[c]	−4289 (35)	6188 (25)	3725 (13)
5N	1942 (8)	2568 (7)	2690 (3)	W7A[a,c]	3402 (29)	4797 (24)	4258 (13)
5CA	927 (10)	2685 (10)	2662 (4)	W7B[a,c]	3785 (42)	5932 (39)	4317 (18)
5CB	404 (9)	2084 (8)	2990 (4)	E1O	−1965 (11)	5193 (10)	2122 (4)
5SG	−844 (3)	2110 (2)	2934 (1)	E1C1	−1402 (20)	4571 (15)	1766 (7)
5OD	−1034 (8)	1624 (6)	2513 (3)	E1C2	−1291 (16)	5142 (13)	1345 (6)
5C	694 (11)	3694 (9)	2698 (4)	E2O[c]	−2619 (28)	2177 (28)	2033 (12)
5O	612 (9)	4145 (6)	2359 (2)	E2C1[c]	−3374 (58)	2611 (60)	2302 (25)
6N	611 (9)	4058 (7)	3086 (3)	E2C2[c]	−3681 (69)	2783 (74)	2174 (26)
6CA	420 (11)	4981 (9)	3148 (4)	E3O[b]	4482 (14)	4148 (13)	2843 (6)
6CB	−548 (10)	5221 (9)	2976 (4)	E3C1[b]	4069 (37)	4729 (33)	2638 (15)
				E3C2[b]	3206 (32)	4807 (29)	2469 (14)

[a] Disordered. [b] Occupancy is 0.50. [c] Occupancy is 0.33. W*n* = water; E*nn* = ethanol. [d] A = α, B = β, G = γ, D = δ, E = ε, Z = ζ, H = η, T = τ. [e] Anisotropic thermal parameters are listed in Kostansek, 1977.

mula approach of direct methods (Germain et al., 1971). A total of 128 phase sets each consisting of those 400 normalized structure factors, $|E|$'s, having $|E| \geq 1.50$, was generated. There were nine reflections in the starting set (the enantiomorph determining reflection had to be chosen by hand) and 3000 triples were utilized in the phase determining process. The five highest absolute figures of merit (Abs FOM) were 1.27, 1.11, 1.09, 1.03, and 1.00. An E map calculated from the phase set with the highest Abs FOM revealed a fragment of the molecule consisting of the peptide backbone and half of the side chains. The remaining side chain atoms were located from an electron density map which was computed from F_o's in the usual way.

Three ethanol molecules and seven water molecules, some of which exhibited considerable thermal motion and distortion, were added to the model by means of successive least-squares refinement cycles and ΔF syntheses. We assigned occupancy values to the solvent molecules based on peak heights in the ΔF maps; these values were held constant during the refinement. The terminal hydroxy group in residue eight occupied three disordered positions.

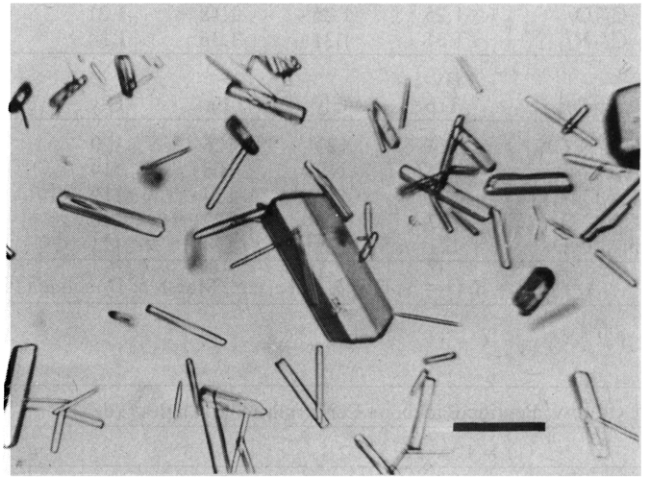

FIGURE 2: Photomicrograph of β-amanitin crystals. The bar represents 1 mm.

TABLE II: Calculated Hydrogen Coordinates × 10^3.

H bonded to atom	x	y	z
1N	−70	402	423
1CA	−131	231	465
1CB	−125	293	371
1CB	−225	255	401
1NE1	−98	14	300
1CE3	−198	95	464
1CZ2	−136	−136	350
1CZ3	−222	−64	480
2N	66	327	408
2CA	169	173	441
2CA	201	283	458
3N	341	188	428
3CA	419	299	363
3CB	476	121	395
3CG1	565	305	413
3CG1	470	262	445
4N	412	296	292
4CA	362	128	245
4CA	392	233	222
5N	228	279	296
5CA	66	246	235
5CB	58	231	332
5CB	64	140	294
6N	68	366	335
6CA	91	542	297
6CB	−55	504	263
6CB	−64	594	301
7CA	132	590	437
7CB	95	739	457
7CB	−26	729	439
7CG	51	818	382
7CD2	80	677	329
7CD2	−37	698	349
8N	−115	560	420
8CA	−128	527	512
8CB	−253	592	460
8CG1	−309	463	528

During the course of refinement it became evident that the data were affected by secondary extinction. Those 40 low angle reflections for which $F_c > F_o$ by $2R$, where the standard crystallographic $R = \Sigma||F_o| - |F_c||/\Sigma|F_o|$, were not included in the final R factor computation. Many of the hydrogens could not be located in the ΔF maps, so calculated hydrogen positions for the 37 nonmethyl hydrogens associated with the peptide molecule were included as constants in the refinement (B = 5 Å^2). Block-diagonal matrix least-squares refinement employing individual anisotropic temperature factors and a fractional weighting scheme (Hughes, 1941) reduced the R to its final value of 10%. A final ΔF map contained no peaks greater than 0.30 e/Å^3. It is possible, however, that there could be more disordered solvent in the structure, but its level would be uninterpretably low. Unfortunately, the crystals were too unstable to determine an experimental density.

Results

Table I contains the positional parameters and estimated standard deviations, for the nonhydrogen atoms in β-amanitin. Table II lists the calculated coordinates of the nonmethyl hydrogen atoms. Among the solvent molecules only the W1 and W2 waters and the E1 ethanol possess an occupancy of unity. The remaining solvent molecules range from 0.50 to 0.33 in fractional population. Water W7 was found to be disordered: its two positions, A and B, are separated by 1.77 Å. This water molecule originally was thought to be ethanol, but it would not refine as ethanol and the electron density distribution was not consistent with the ethanol geometry. The E2 and E3 ethanols are somewhat distorted because the complex positional disorder exhibited in the ΔF maps could not be reproduced with simple disorder models. The oxygens in these molecules were identified by peak height and proximity to possible hydrogen bonding groups.

Table III lists the backbone bond lengths and angles. Average values of these parameters compare favorably with ac-

TABLE III: Backbone Bond Lengths (Å) and Angles (deg).[a]

bonds	i = 1	2	3	4	5	6	7	8	av i = 1–8	av for polypeptides[b]
N_i–CA_i	1.43	1.38	1.45	1.50	1.43	1.42	1.48	1.41	1.44	1.455
CA_i–C_i	1.50	1.48	1.56	1.48	1.55	1.60	1.48	1.55	1.52	1.51
C_i–O_i	1.25	1.26	1.18	1.21	1.25	1.22	1.26	1.26	1.24	1.24
C_i–N_{i+1}	1.31	1.31	1.36	1.34	/32	1.35	1.30	1.33	1.33	1.325
angles	Hy-Trp	Gly	Ile	Gly	Cys	Asp	Hyp	DiHy-Ile		
$C_{i-1}N_iCA_i$	124	123	126	120	124	122	117	123	122	122
$N_iCA_iC_i$	114	119	108	114	109	105	115	112	112	111
$CA_iC_iN_{i+1}$	121	118	114	119	119	118	116	117	118	116
$CA_iC_iO_i$	117	118	122	120	119	120	116	121	119	120.5
$N_{i+1}C_iO_i$	121	123	124	121	122	122	122	123	122	123.5

[a] A = α, B = β, G = γ, D = δ. [b] See, e.g., Marsh & Donohue (1967).

TABLE IV: Peptide Backbone Conformational Angles[a] (deg) for β-Amanitin X-ray.

	i = 1	2	3	4	5	6	7	8
ϕ_i	109	140	−59	87	−121	−172	−60	−79
ψ_i	−40	−178	127	−4	−85	179	−37	−23
ω_i	172	−175	−176	−173	178	−174	−172	−169

[a] Using the conventions set forth by IUPAC-IUB Commission on Biochemical Nomenclature (1970).

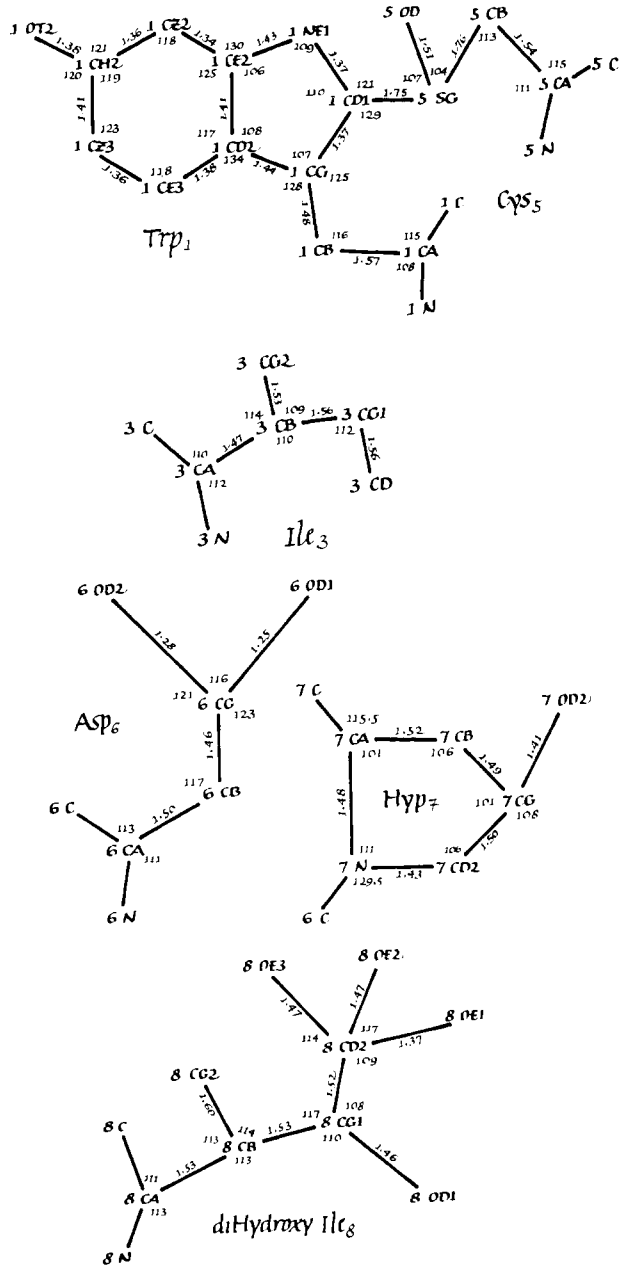

FIGURE 3: Bonds and angles of side chains.

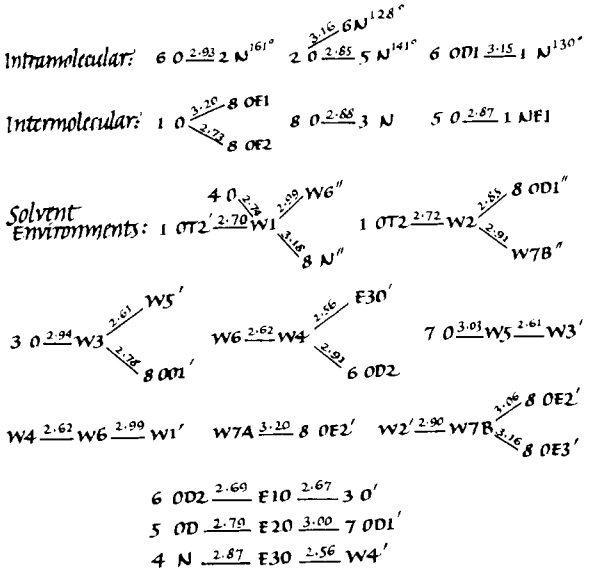

FIGURE 5: Hydrogen bond contact distances less than 3.21 Å.

cepted (Marsh & Donohue, 1967) polypeptide backbone distances and angles. A few individual values deviate significantly from the mean, but these are not outside of the range observed in other polypeptide crystal structures. Estimated standard deviations for the backbone parameters are less than 0.10 Å for the lengths and 1.0° for the angles. In addition to the distances and angles, Figure 3 illustrates the side chain labeling scheme. The geometry of the terminal hydroxyl group in residue eight is somewhat distorted because of the threefold disorder. Peptide torsion angles (IUPAC-IUB, 1970) for β-amanitin are listed in Table IV. All of the peptide bonds assume the trans conformation. The average deviation from ideal trans is 6.4°, whereas 11° is the maximum deviation. The Hyp[7] residue has a C_s–C_γ exo ring conformation (Ashida & Kakudo, 1974).

Figure 4 is a computer-generated stereoscopic view (Johnson, 1965) of the molecule. At the right of the molecule there is a single turn which is very nearly α helical. The structure is "T" shaped and possesses two 18-membered rings. Two 13-atom segments of the peptide backbone are approximately perpendicular to each other (thus forming an "L" shape for the octapeptide ring itself).

A rather extensive hydrogen-bonding scheme exists in the β-amanitin crystal structure. Figure 5 identifies the hydrogen bond type interactions of less than 3.21 Å separation. Two fairly strong and two very weak intramolecular interactions take place at the peptide ring turns. At one turn there is the 5 → 1 H-bond between 6O and 2N, and the weak side chain to backbone interaction of 6OD1 (of Asp[6]) to 1N. At the other turn one finds both 4 → 1 and 5 → 1 (weak) interactions from 2O to 5N and 6N, respectively. This latter hydrogen-bonding relationship is similar to one found in the crystal structure (Iitaka et al., 1974) of the cycloheptapeptide ilamycin B_1. Three fairly strong intermolecular H bonds directly connect the cyclopeptides in the crystal. These are 1O to 8O E2′, 8O to 3N′, and 5O to 1NE1′. As can be seen from Figure 4, most

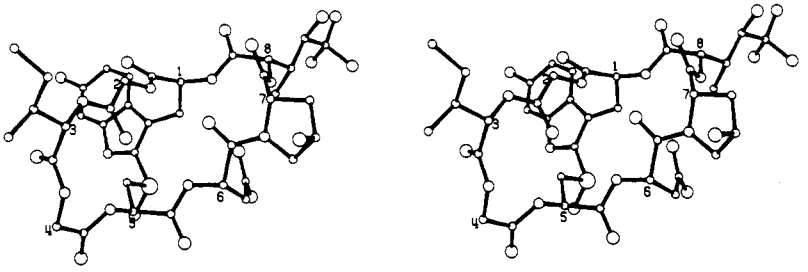

FIGURE 4: Stereoview of β-amanitin molecule. The three atoms at the far right represent the disordered positions of the terminal hydroxyl in residue 8.

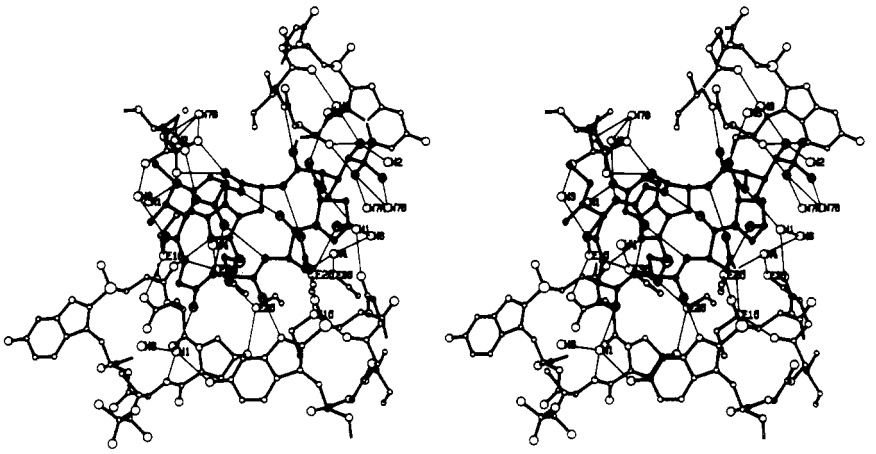

FIGURE 6: Stereoview of toxin environment in the crystal showing the hydrogen-bonding scheme.

of the solvent molecules serve as bridges between adjacent β-amanitin molecules. The large amount of solvent provides "filler" between the irregularly shaped cyclopeptides. Virtually every possible group is hydrogen bonded in this structure. Figure 6 is a stereoscopic view showing packing of the toxin molecule and its surroundings in the crystal.

Discussion

The crystallographic results confirm the latest chemical structural work assigning the *R* configuration to the C_β and C_γ atoms dihydroxyisoleucine (Gieren et al., 1974) and to the sulfur of the cysteine (Wieland et al., 1974; Faulstich et al., 1968). In addition, the configuration at the C_γ atom of the hydroxyproline is established as *R*. All amino acid residues have the L configuration and the C_β atom of the isoleucine is *S* as expected.

There are several examples in the literature where β-amanitin has been coupled to bovine serum albumin via a carbodiimide activated amide bond (Fiume et al., 1971; Cessi & Fiume, 1969). The yield of carbodiimide promoted reactions is ordinarily quantitative (Carraway et al., 1969) but only 2.5% of the β-amanitin was coupled to bovine serum albumin under the conditions tested (Fiume et al., 1971). Thus it appeared that the free carboxyl group of the aspartic acid residue in the toxin is rather unreactive. This lack of reactivity can be explained by the finding that the carboxylic acid in question is hydrogen bonded and tucked in toward the center of the molecule, causing it to be sterically hindered.

It has been suggested (Cochet-Meilhac & Chambon, 1974) that hydrogen bonding seems to play an important role in the amatoxin–RNA polymerase II complex stability and that hydrophobicity could facilitate the formation of the complex. The crystal structure contains two distinct regions which may be related to these proposals. The cross bar of the "T"-shaped toxin possesses great potential for hydrogen bonding. This section contains four hydroxyls, a carboxylic acid, an indole N–H, and a sulfoxide. By contrast, the stem of the "T" contains only the hydrophobic residues Gly^2, Ile^3, and Gly^4. Perhaps these separate parts of the molecule contribute cooperatively to the action of the toxin.

Due to the fairly rigid bicyclic ring system and the presence of so much solvent in the crystal, we feel that the crystal conformation is probably similar to the conformation found in aqueous solution. Circular dichroism studies (Faulstich et al., 1973) of the biologically active amatoxins in water and methanol show little conformational variation among the various toxins. From this and other studies (Cochet-Meilhac & Chambon, 1974; Buku et al., 1971), it seems likely that the overall conformation of the amatoxins is of great importance for the binding to and inhibition of RNA polymerase II.

Acknowledgment

The purification and crystallization of β-amanitin were performed in the laboratory of Jack Strominger with support from National Institutes of Health Grant AM-13230. Donald M. Simons' expert knowledge of poisonous mushrooms was an essential contribution.

References

Ashida, T., & Kakudo, M. (1974) *Bull. Chem. Soc. Jpn. 47,* 1127.

Buku, A., Campadelli-Fiume, G., Fiume, L., & Wieland, T. (1971) *FEBS Lett. 14,* 42.

Carraway, K., Spoerl, P., & Koshland, D. (1969) *J. Mol. Biol. 42,* 133.

Cessi, C., & Fiume, L. (1969) *Toxicon 6,* 309.

Cochet-Meilhac, M., & Chambon, P. (1974) *Biochim. Biophys. Acta 353,* 160.

Faulstich, H., & Weckauf-Bloching, M. (1974) *Hoppe-Seyler's Z. Physiol. Chem. 355,* 1489.

Faulstich, H., Wieland, T., & Jocham, C. (1968) *Justus Liebigs Ann. Chem.,* 186.

Faulstich, H., Bloching, M., Zobeley, S., & Wieland, T. (1973) *Experientia 29,* 1230.

Fiume, L., Campadelli-Fiume, G., & Wieland, T. (1971) *Nature (London), New Biol. 230,* 220.

Germain, G., Main, P., & Woolfson, M. (1971) *Acta Crystallogr., Sect. A 27,* 368 (the figure of merit is defined on p 374 of this reference).

Gieren, A., Narayanan, P., Hoppe, W., Hasan, M., Michl, K., Wieland, T., & Smith, H. (1974) *Justus Liebigs Ann. Chem.,* 1561.

Hughes, E. (1941) *J. Am. Chem. Soc. 63,* 1737.

Iitaka, Y., Nakamura, H., Takada, L., & Takita, T. (1974) *Acta Crystallogr., Sect. B 30,* 2871.

IUPAC-IUB Commission on Biochemical Nomenclature (1970) *Biochemistry 9,* 3471.

Johnson, C. (1965) ORTEP, ORNL-3794, Oak Ridge National Laboratory, Oak Ridge, Tenn.

Kostansek, E. (1977) Ph.D. Thesis, Harvard University, Cambridge, Mass.

Kostansek, E., Lipscomb, W. N., Yocum, R., & Thiessen, W. (1977) *J. Am. Chem. Soc. 99,* 1273.

Marsh, R., & Donohue, J. (1967) *Adv. Protein Chem. 22,* 235.
Wieland, T., & Gebert, U. (1966) *Justus Liebigs Ann. Chem. 700,* 157.
Wieland, T., & Wieland, O. (1972) in *Microbial Toxins,* Vol. 8 (Kadis, S., Cigler, A., & Ajl, S., Eds.) pp 249–280, Academic Press, New York, N.Y.
Wieland, T., Wirth, L., & Fischer, E. (1949) *Justus Liebigs Ann. Chem. 564,* 152.
Wieland, T., de Urries, M., Indest, H., Faulstich, H., Gieren, A., Strum, M., & Hoppe, W. (1974) *Justus Liebigs Ann. Chem.,* 1570.
Yocum, R. R. (1978) *Biochemistry 17* (preceding paper in this issue).

Mode of Coupling between the β-Adrenergic Receptor and Adenylate Cyclase in Turkey Erythrocytes†

Aviva M. Tolkovsky and Alexander Levitzki*

ABSTRACT: The mode of coupling of the β-adrenergic receptor to the enzyme adenylate cyclase in turkey erythrocyte membranes was analyzed in detail. A number of experimental techniques have been used: (1) measurement of the kinetics of cyclase activation to its permanently active state in the presence of guanylyl imidodiphosphate, as a function of hormone concentration; (2) measurement of antagonist and agonist binding to the β-adrenergic receptor prior and subsequent to the enzyme activation by hormone and guanylyl imidodiphosphate. On the basis of these two approaches, all the models of receptor to enzyme coupling which involve an equilibrium between the enzyme and the receptor can be rejected. The binding and the kinetic data, however, can be fitted by two diametrically opposed models of receptor to enzyme coupling: (a) the precoupled enzyme-receptor model where activation of the enzyme occurs, according to the following scheme:

$$H + RE \underset{k_2}{\overset{k_1}{\rightleftharpoons}} HRE \xrightarrow{k} HRE' \qquad (1a)$$

where H is the hormone, RE is the precoupled receptor–enzyme complex, k_1 and k_2 are the rate constants describing hormone binding, and k is the rate constant characterizing the formation of HRE′ from the intermediate HRE. According to this model, the activated complex is composed of all of the interacting species. (b) The other model is the collision coupling mechanism:

$$H + R \underset{K_H}{\rightleftharpoons} HR + E \xrightarrow{k_1} HRE \xrightarrow[k_3]{} HR + E' \qquad (1b)$$

where K_H is the hormone–receptor dissociation constant, k_1 is the bimolecular rate constant governing the formation of HRE, and k_3 the rate constant governing the activation of the enzyme. In this case the intermediate never accumulates and constitutes only a small fraction of the total receptor and adenylate cyclase concentrations. In order to establish which of the two mechanisms governs the mode of adenylate cyclase activation by its receptor, a diagnostic experiment was performed: Progressive inactivation of the β receptor by a specific affinity label was found to cause a decrease in the maximal binding capacity of the receptor and a proportional decrease in the rate of activation, but no change in the maximum level of activity was attained. Progressive inactivation of the enzyme by *p*-hydroxymercuribenzoate was found not to change the rate of activation nor the capacity of the receptor to bind hormone. Only the maximal level of activation was found to be decreased. These results are not compatible with the precoupled model of receptor and cyclase nor with floating receptor models in which an intermediate of hormone, receptor, and cyclase is in equilibrium with its reactants. The data strongly suggest that the collision coupling is the mode of coupling between the β receptor and cyclase coupling in turkey erythrocyte membranes.

In the Appendix we have described five different molecular models for receptor to enzyme coupling. In this manuscript we present an attempt to analyze completely the mechanism of receptor to adenylate cyclase coupling in turkey erythrocyte membranes.

Turkey erythrocyte membranes possess an adenylate cyclase coupled to β-adrenergic receptors capable of being stimulated by l-catecholamines (Davoren and Sutherland, 1963). One of the major problems concerning the cyclase–receptor complex is the mechanism by which hormone binding to the receptor induces the activation of adenylate cyclase. An intriguing aspect of cyclase activation by hormones concerns the permanently active enzyme which is formed in the presence of hormone and GppNHp[1] (Schramm and Rodbell, 1975; Pfeuffer and Helmreich, 1975; Sevilla et al., 1976; Levitzki et al., 1976; Spiegel et al., 1976). Although the highly active state is induced by hormone and therefore must be formed through interaction with the receptor, once formed this state

† From the Department of Biological Chemistry, The Hebrew University of Jerusalem, Jerusalem, Israel. *Received September 12, 1977; revised manuscript received March 9, 1978.* This work was supported by a grant from the U.S.–Israel Binational Research Foundation, Jerusalem, Israel.

[1] Abbreviations used are: PEP, phosphoenolypyruvate; PPL, propranolol; PHMB, *p*-hydroxymercuribenzoate; NHNP-NBE, *N*-[2-hydroxy-3-(1-naphthyloxy)propyl-*N*′-bromoacetylethylenediamine]; TME, 50 mM Tris, 2 mM $MgCl_2$, 1 mM EDTA, pH 7.4, buffer; HYP, hydroxybenzylpindolol; Tris, 2-amino-2-hydroxymethyl-1,3-propanediol; EDTA, (ethylenedinitrilo)tetraacetic acid; GppNHp, guanylyl imidodiphosphate.

0006-2960/78/0417-3795$01.00/0